30th Annual International IEEE EMBS Conference
Vancouver, British Columbia, Canada, August 20-24, 2008

Abnormalities in MRI traits of Corpus Callosum in Autism Subtype

Qing He, Kevin Karsch, and Ye Duan

Abstract—**A number of studies have documented that autism has a neurobiological basis, but the anatomical extent of these neurobiological abnormalities is largely unknown. In this paper, we apply advanced computational techniques to extract 3D models of the corpus callosum (CC) and subsequently analyze the volumetric deficit of the total CC and its five sub-regions in a homogeneous group of autistic children. Moreover, we explore new MRI traits based on the oriented bounding rectangle of the CC, which are the length, width and aspect ratio of the bounding rectangle. These measurements as well as the volumes are compared between patients and controls using t-tests. The results reveal significant reduction in all sub-regions of the CC and some MRI traits in the patients.**

I. Introduction

A number of studies have documented that autism has a neurobiological basis, but the anatomical extent of these neurobiological abnormalities is largely unknown [1]. Several studies have reported deficits in the size of the corpus callosum (CC) and its subregions, although the results are inconsistent with regard to CC subregions. For example, [2] reported reductions in the size of the body and posterior regions of the CC in autistic patients, [7] found significant differences in anterior regions, and [1] found reductions in genu and splenium as well as the total CC area. A detailed summary of CC abnormalities in autism can be found in [8]. The inconsistency of the results may be due to factors such as the sample size, subject age and gender, and specific diagnosis. Particularly, heterogeneity within the autism diagnosis obscures the genetic basis of the disorder [5]. Recently, Miles et al. proposed a new definition of autism subgroups, which divided autism into essential autism and complex autism [5]. Limiting studies of brain morphology to individuals with essential autism decreases the background noise of structural variation and allow the analysis of the more uniform population [5]. He et.al [16] first adopted this definition and compared the shape difference between subjects with essential autism and controls, although their sample size was conspicuously small. In this paper, we also focus on essential autism, which will greatly reduce the heterogeneous factors.

Quantitative morphologic assessment of individual brain structures is often based on volumetric measurements and shape analysis [6]. Volume comparison gives global information of the size difference between pathological and healthy structures, but no local shape difference is revealed. On the contrary, shape analysis [4,6] can precisely locate morphological changes in pathological structures, but it gives little global information of the difference between two groups of structures. In this paper, we explore several MRI traits of the corpus callosum as well as the volume. An MRI trait is a phenotypic trait [11] of an organism on MR images. An oriented bounding rectangle of the 2D corpus callosum on sagittal MRI is constructed, and the length, width and ratio (length/width) of the bounding rectangle are the MRI traits to be compared between autism and control groups. Since the oriented bounding rectangle of an object is the minimum rectangle that encloses this object, the measurements of the bounding rectangle can give both size and shape information.

Traditional volume analysis is also performed in a way similar to [1]. Volumes of the entire CC and five sub-regions are compared. CC thickness at each region border is also compared. The 3D model of the CC is reconstructed from 2D contours of nine sagittal slices as in [1]. We use a newly developed semiautomatic method [9] to segment the CC from 2D MR images, which is faster and more accurate than manual segmentation. The results of this paper show the differences in the volumes and MRI traits between patients and controls.

II. Methods

A. CC Modeling

We start with slice-by-slice segmentation and stack the 2D curves to make a 3D model. Because it is more straightforward to verify the accuracy of 2D results slice by slice, this method provides better results as opposed to direct 3D segmentation and validation. Mid-sagittal slice and four adjacent slices on each side are used for CC segmentation. We use the semiautomatic method proposed by He et.al [9] to segment the CC on sagittal slices, which is faster and more accurate than manual segmentation. The user initializes a polyline inside the CC region by three mouse clicks (Fig. 1(a)), and a seed contour consisting of four parts is automatically generated by point tracing on the edge map (Fig. 1(b), (c)). The seed will then automatically deform according to active contour evolution, but each part has its own motion law. The contour evolution mechanism can be

Manuscript received March 23, 2008. This work was supported in part by the Shumaker Biomedical Informatics fellowship and NIH training grant for training Clinical Biodetectives.

Qing He is with the Department of Computer Science, University of Missouri-Columbia, Columbia, MO, 65211 USA (phone: 573-882-3842; fax: 303-882-8318; e-mail: qhgb2@mizzou.edu).

Kevin Karsch is with the Department of Computer Science, University of Missouri-Columbia, Columbia, MO, 65211 USA (e-mail: krkq35@mizzou.edu).

Ye Duan is with the Department of Computer Science, University of Missouri-Columbia, Columbia, MO, 65211 USA (e-mail: duanye@missouri.edu).

found in [9]. The fornix tip can also be removed by automatic fornix detection [9]. The final result on one sagittal slice is shown in Fig. 1(d). Since the CC shapes on adjacent slices do not differ too much, we apply the segmentation method on mid-sagittal slice and the result is used as the seed for its two neighbor slices. After slight deformation the boundary curves on these two slices can be obtained and each one is again used as the seed of its next adjacent slice.

Contour stitching is performed to create the 3D CC model of each subject. Since the segmentation method can keep track of the four parts of the CC boundary, the point correspondence problem can be simplified by first matching the sensor points among contours [16]. After matching the sensor points, the four parts are implicitly matched among contours. We only need to match the individual points within each part. The details of matching the sensor points and the inner points of the four parts can be found in [16]. By connecting the matched point pairs between adjacent contours, the 3D mesh is created. A tangential Laplacian smoothing [12] is performed to maintain a good node distribution of the model.

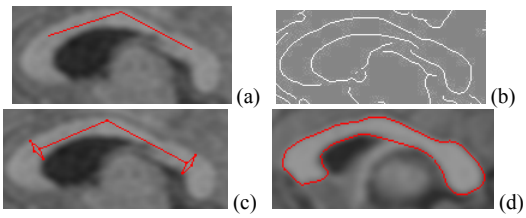

Fig.1 (a) User-initialized polyline. (b) The edge map. (c) The completed seed contour. (d) The final result

B. Volume Measurements

Volumes of the CC and its sub-regions are computed similar to that in [1]. We first find the farthest two points p1 and p2 on the CC boundary, and then divide the CC into five regions along line p1p2 (Fig.2(a)). The five regions are defined the same as in [1]. For simplicity, we label them from r1 to r5 as shown in Fig.2(a). Areas are computed in pixels for each 2D segmented CC, and the areas of 9 slices are summed to generate the voxel count of the 3D model. The raw volume is the multiplication of the voxel count and the voxel size in mm^3. To take into account the effect of the brain volume, we normalize the raw CC volume by the total brain volume (TBV) and the intracranial volume (ICV) respectively. TBV includes grey matter and white matter and excludes ventricles [14], and ICV is the sum of white matter, grey matter, and inner and outer cerebrospinal fluid spaces [13]. A choice can be made between using TBV or ICV as an adjustment factor [14], but our results show that the two choices do not make any difference. The brain volumes, raw and scaled volumes of the CC and the five regions are compared between patients and controls using t-tests.

C. MRI Traits

We explore MRI traits based on the oriented bounding rectangle of the CC. To construct the rectangle, we first find points p1 and p2 as mentioned above. On each side of line p1p2, we find a point on the CC boundary which has the maximum distance to line p1p2 (p3, p4 in Fig.2(b)). The bounding box is a rectangle whose long edges pass p3 and p4 respectively and are parallel to line p1p2, and whose short edges pass p1 and p2 respectively (Fig.2(b)). We measure the length, width, and aspect ratio (length/width) of the bounding rectangle on each 2D slice and average them across the 9 slices. The shape of the bounding box depends on both the size and the shape of the CC, so these MRI traits can reflect both size and shape information of the CC. We also compute the thickness at the border of every two sub-regions, which is the length of each dividing line (L1~L4 in Fig.2(a)). With a little abuse of notation, we denote the thickness at each dividing border as L1~L4. The thickness at each border is averaged across the 9 slices. The average measurements of the bounding box and the thickness are compared between patients and controls using t-tests.

To account for the brain volume effect, we scale the above raw measurements by the cubic root of TBV and ICV respectively. Since these measurements are in mm, this scaling makes the units consistent. These scaled measurements are also compared between patients and controls.

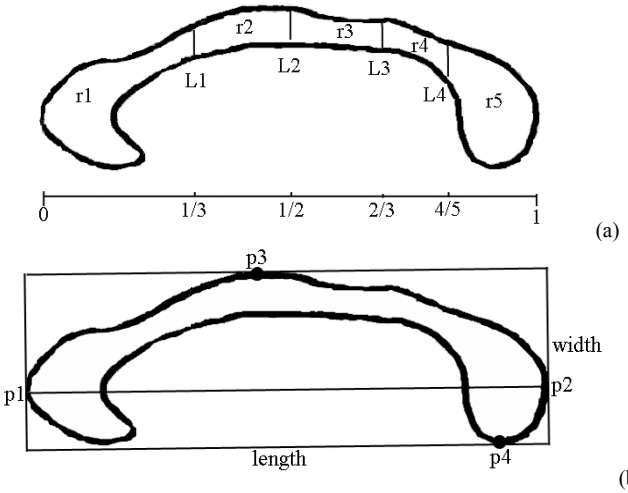

Fig.2 (a) partition of the CC: r1—anterior third; r2—anterior body; r3—posterior body; r4—isthmus; r5—splenium. (b) oriented bounding rectangle of the CC

III. Results

30 patients with essential autism participated in this study. All patients met the DSM-IV criteria [10] as well as Autism Diagnostic Interview-Revised (ADI-R) and ADOS algorithm criteria. The distinction between essential and complex autism is based on the presence of generalized dysmorphology which is indicative of an insult to early embryologic development and has been previously reported [5]. Children with a known disorder such as Fragile X, Tuberous Sclerosis, a chromosome abnormality or severe prematurity with brain damage and children with IQs/DQs less than 40 will be excluded. 5 healthy people recruited from the NIH Human Brain Project participated as controls.

Besides, we also obtained MR images of 23 controls from IBSR database [15]. The age range of all participants is 3~30. Both groups include males and females at roughly equal number.

MR images of our patients and controls were obtained from our autism aesthesia protocol which included intravenous infusion of protocol to ensure image quality. Axial, coronal and sagittal T1-weighted images were acquired using the Siemens Symphony 1.5 T scanner with the following parameters: TR = 35ms, NEX = 1, flip-angle = 30 degrees, thickness = 1.5mm, field of view = 22cm, matrix =512x512. The data obtained from IBSR were T1-weighted MR images with 3.1mm thickness. Each brain volume was interpolated to 0.9-mm isotropic voxels to balance between computational cost and data quality.

Table 1 shows the t-test results of the volumes. The mean TBV and ICV of the patients are greater than those of the controls, but the p-values do not reveal any significance in this difference ($p>0.05$). The raw measures of the CC volume and its sub-regions all show that the patient's volume is significantly smaller than the controls ($p<=0.05$), especially in the region r2 (anterior body). The comparison of the scaled measures by TBV and by ICV shows similar results, both of which augment the significance of the difference. Table 1 only shows the results of TBV normalization.

Table 2 gives the t-test results of the MRI traits regarding the bounding rectangle and the thickness. In the raw measures, the patients have significantly reduced length and aspect ratio of the bounding rectangle, while other traits do not show any significance in the difference between patients and controls. When scaled by the cubic root of TBV, the length of the bounding rectangle keeps its strong significance and the width still shows no significance in the group difference. The p-values of the difference in thickness are decreased but none of them reach the significance level (0.05). The difference in L2 between patients and controls is close to significant, which is consistent with the volume measurements since the anterior body displays most significant difference. The comparison shows similar results when the measurements are scaled by the cubic root of ICV, and Table 2 only shows the results of TBV normalization.

TABLE I
VOLUME MEASUREMENTS

CC Measure	Patients	Controls	p-value
TBV (cm^3)	1421.9±299.4	1313.6±336.0	0.09
ICV (cm^3)	1460.4±308.3	1348.3±345.5	0.09
Raw measures	(mm^3)		
Total CC	4229.1±755.3	4727.7.0±971.4	0.01
r1	1754.2±321.3	1939.5±367.9	0.02
r2	474.4±103.9	556.1±142.9	0.008
r3	439.7±123.1	505.1±139.9	0.03
r4	404.6±108.3	458.8±140.8	0.05
r5	1153.3±227.7	1263.5±275.7	0.05
Scaled by TBV	($\times 10^{-4}$)		
Total CC	31.0±9.3	37.0±8.1	0.004
r1	13.0±3.5	15.1±3.1	0.004
r2	3.4±1.0	4.3±1.0	0.001
r3	3.2±1.2	3.9±1.0	0.009
r4	2.9±1.0	3.6±0.9	0.01
r5	8.6±2.9	10.1±2.4	0.02

TABLE II
MRI TRAITS

CC Measure	Patients	Controls	p-value
Raw measures	(mm)		
Length	66.2±4.8	72.1±5.0	$<10^{-4}$
Width	24.0±3.0	23.6±3.6	0.33
Length/width	2.78±0.3	3.11±0.49	0.002
L1	5.91±1.13	6.09±1.19	0.28
L2	5.40±1.18	5.76±1.35	0.14
L3	5.11±1.35	5.29±1.53	0.31
L4	7.53±1.76	7.77±2.06	0.32
Scaled by TBV			
Length	0.59±0.05	0.66±0.06	$<10^{-4}$
Width	0.21±0.02	0.22±0.03	0.35
L1	0.053±0.011	0.056±0.010	0.14
L2	0.048±0.011	0.053±0.011	0.07
L3	0.045±0.012	0.048±0.013	0.20
L4	0.067±0.016	0.071±0.017	0.22

IV. CONCLUSION

Based on the new definition of autism subgroups, we investigate the CC abnormalities in essential autism, and exclude the complex autism group in order to find more homogeneous results. We use a semiautomatic method to segment 2D CC boundaries, and 3D surfaces are reconstructed by contour stitching. Regional volumes and MRI traits of the CC are measured and scaled by TBV and ICV. Both raw and scaled measurements are compared between patients and controls using t-tests.

In the volume comparison, no significance is found in TBV or ICV between patients and controls, but the non-significant trend for an increase in the brain volumes in patients is consistent with most previous literatures [2,3,7]. The significant reduction in the total CC volume in the patients is consistent with [1]. We find significant reduction in each sub-region of the CC in the patients, but in [1] only a significant reduction in the anterior third was found. Besides the traditional volume test, we also conduct some tests based on the oriented bounding rectangle, which has not been done in previous work. The length, width, and aspect ratio of the bounding rectangle are measured for comparison. We find significant reduction in the CC length and ratio in the patients, but the difference in the width is far from significant. This gives us some insight that the decrease in the CC volume is caused by the decrease in the anterior-posterior length more than the top-bottom length.

The results of this study need to be interpreted cautiously because of several limitations. First of all, the age range of our sample is very wide, which may have some effect on the CC measurements. Secondly, we exclude the complex autism group. Further studies on different subgroups within autistic patients need to be done, such as male vs. female, and complex vs. essential. These findings will better explain the inconsistent results caused by the population.

REFERENCES

[1] C. N. Vidal, R. Nicolson, T. J. DeVito, K. M. Hayashi, J. A. Geaga, D. J. Drost, P. C. Williamson, N.Rajakumar, Y. Sui, R. A. Dutton, A.W.

Toga, and P.M. Thompson, "Mapping corpus callosum deficits in autism: an index of aberrant cortical connectivity", *Biological Psychiatry*, 60(3), 2006, pp. 218-225.

[2] J. Piven, J. Bailey, B. J. Ranson, and S. Arndt, "An MRI study of the corpus callosum in autism", *Am J Psychiatry*, vol. 154, 1997, pp. 1051-1056.

[3] S. L. Palmer, W. E. Reddick, J. O. Glass, A.Gajjar, O. Goloubeva, and R. K. Mulhern, "Decline in corpus callosum volume among pediatric patients with medulloblastoma: longitudinal MR imaging study", *AJNR Am J Neuroradiol*, vol. 23, 2002, pp. 1088–1094

[4] R. Nicolson, T.J. Devito, C.N. Vidal, Y. Sui, K.M. Hayashi, D.J. Drost, P.C. Williamson, N. Rajakumar, A.W. Toga, and P.M. Thompson, "Detection and mapping of hippocampal abnormalities in autism", *Psychiatry Research: Neuroimaging*, vol.148, 2006, pp. 11-21

[5] J.H. Miles, T.N. Takahashi, S. Bagby, P.K. Sahota, D.F. Vaslow, C.H. Wang, R.E. Hillman, and J.E. Farmer, "Essential vs Complex Autism: Definition of Fundamental Prognostic Subtypes", *Am. J. Medical Genetics*, vol. 135A, 2005, pp.171-180

[6] M. Styner, L. Oguz, S. Xu, C. Brechbuehler, D. Pantazis, J.J. Levitt, M.E. Shenton, and G. Gerig, "Framework for the Statistical Shape Analysis of Brain Structures using SPHARM-PDM", *ISC/NA-MIC Workshop on Open Science at MICCAI*, 2006

[7] A.Y. Hardan, N.J. Minshew, and M.S. Keshavan, "Corpus callosum size in autism", *Neurology*, vol. 55, 2000, pp. 1033–1036

[8] P. Brambilla, A. Hardan, S. Ucelli di Nemi, J. Perez, J.C. Soares, and F. Barale, "Brain anatomy and development in autism: review of MRI studies", *Brain Research Bulletin*, vol. 61, 2003, pp. 557-569

[9] Q. He, Y. Duan, JH. Miles, N. Takahashi, "A Context-Sensitive Active Contour for Image Segmentation", *International Journal of Biomedical Imaging*, vol. 2007, Article ID 24826, 8 pages, 2007. doi: 10.1155/2007/24826

[10] American Psychiatric Association, *Diagnostic and Statistical Manual of Mental Disorders*, 4th ed., text revision, American Psychiatric Association, Washington DC, 2000

[11] C.Shyu, JM.Green, DPK. Lun, T. Kazic, M.Schaeffer, and E.Coe. "Image Analysis for Mapping Immeasurable Phenotypes in Maize", *IEEE Signal Processing Magazine*, May, 2007: 115-118

[12] Z. Wood, M. Desbrun, P. Schroder, and D. Breen, "Semi-Regular Mesh Extraction from Volume", *Proceedings of the conference on Visualization*, 2000: 275 – 282

[13] H. Wolf, F. Kruggel, A. Hensel, L. Wahlund, T. Arendt and H. Gertz, "The relationship between head size and intracranial volume in elderly subjects", *Brain Research* 973(1), 2003, pp. 74-80

[14] L.M. O'Brien, D.A. Ziegler, C.K. Deutsch, D.N. Kennedy, J.M. Goldstein, L.J. Seidman, S. Hodge, N. Makris, V. Caviness, J. A. Frazier, M. R. Herbert, "Adjustment for Whole Brain and Cranial Size in Volumetric Brain Studies: A Review of Common Adjustment Factors and Statistical Methods", *Harvard Review of Psychiatry*, 14(3), 2006, pp.141 - 151

[15] http://www.cma.mgh.harvard.edu/ibsr/

[16] Q. He, Y. Duan, JH. Miles, TN. Takahashi, "Statistical Shape Analysis of the Corpus Callosum in Subtypes of Autism", *IEEE 7th International Symposium on Bioinformatics & Bioengineering*, Boston, Massachusetts, USA, Oct 14-17, 2007